Heterogeneous Elasticity: The tale of the boson peak

Walter Schirmacher[1] and Giancarlo Ruocco[2,3]
[1] *Institut für Physik, Universität Mainz, Staudinger Weg 7, D-55099 Mainz, Germany*
[2] *Fondazione Istituto Italiano di Tecnologia (IIT), Center for Life Nano Science, Viale Regina Elena 291, I00161 Roma, Italy and*
[3] *Department of Physics, University of Rome 'La Sapienza', Piazzale Aldo Moro, 5, I00185, Rome, Italy*

The vibrational anomalies of glasses, in particular the boson peak, are addressed from the standpoint of heterogeneous elasticity, namely the spatial fluctuations of elastic constants caused by the structural disorder of the amorphous materials.

In the first part of this review article a mathematical analogy between diffusive motion in a disordered environment and a scalar simplification of vibrational motion under the same condition is emploited. We demonstrate that the disorder-induced long-time tails of diffusion correspond to the Rayleigh scattering law in the vibrational system and that the cross-over from normal to anomalous diffusion corresponds to the boson peak. The anomalous motion arises as soon as the disorder-induced self-energy exceeds the frequency-independent diffusivity/elasticity. For this model a variational scheme is emploited for deriving two mean-field theories of disorder, the self-consistent Born approximation (SCBA) and coherent-potential approximation (CPA). The former applies if the fluctuations are weak and Gaussian, the latter applies for stronger and non-Gaussian fluctuations.

In the second part the vectorial theory of heterogenous elasticity is presented and solved in SCBA and CPA, introduced for the scalar model. Both approaches predict and explain the boson-peak and the associated anomalies, namely a dip in the acoustic phase velocity and a characteristic strong increase of the acoustic attenuation below the boson peak. Explicit expressions for the density of states and the inelastic Raman, neutron and X-ray scattering laws are given. Recent conflicting ways of explaining the boson-peak anomalies are discussed.

I. INTRODUCTION

The vibrational properties of disordered solids are quite different from those of crystals [1, 2]. While the harmonic vibrational spectra of crystals are given by the dispersion relations obtained from the crystalline symmetry groups, those of amorphous solids, in particular glasses exhibit anomalous, continuous spectra, which are a matter of debate since 60 years [2–7].

The first evidence of something unusual in the vibrational spectra of glasses came from Raman scattering [8–13]. In the THz or 100 wavenumber regime one observed a broad maximum, where usually either no intensity or very sharp peaks due to low-lying optical modes were observed. Because this maximum obeyed the frequency/temperature dependence of the Bose function $n(\omega)+1 = [1-exp\{-\hbar\omega/k_BT\}]^{-1}$ ($\omega/2\pi$ is the frequency and k_BT is the Boltzmann constant times the temperature) one called this maximum "boson peak" [14]. Here we note that because the Raman scattering intensity is proportional to $n(\omega)+1$ times the Raman spectral function $\chi''_R(\omega)$ [13, 15, 16], the latter must be temperature independent if the entire temperature dependence comes from the Bose function. This points to a harmonic origin of the boson peak and questions all interpretations in terms of anharmonic interactions.

A maximum in the frequency range $\sim$ 5 meV $\sim$ 1 THz was observed in inelastic coherent neutron scattering data of several glasses [17]. This maximum appeared to be related to an excess of the vibrational density of states (DOS) $g(\omega)$ with respect to Debye's $g(\omega) \propto \omega^2$ law, which appears as a peak in the reduced DOS $g(\omega)/\omega^2$. This was confirmed experimentally by means of inelastic incoherent neutron [18] and nuclear scattering [19], which both measures directly the DOS. Further, the boson peak turned out to be related to a maximum in the "reduced" specific heat $C(T)/T^3$ in the 10K regime [18, 20], which is also called "boson peak". Right at the boson-peak temperature the thermal conductivity of the same glasses exhibits a characteristic shoulder or dip in its temperature dependence [21], which turned out to be an "upside-down boson peak" [22].

These are not the only low-temperature thermal anomalies of glasses. Below the boson peak, in the $\sim$ 1K regime, the specific heat does not show Debye's T^3 law, but varies approximately linearly with temperature. The thermal conductivity varies quadratically in this regime. These findings have been attributed to the existence of bistable structural arrangements, which allow for tunneling between the two positions, giving rise to a tunnel splitting (two-level systems (TLS), tunneling systems) [23–27]. If the energy separations of the TLS are assumed to have a broad distribution, the 1K anomalies can be explained. Independent evidence for the existence of the TLS comes from ultrasonic and nuclear magnetic resonance data [28, 29].

Inelastic X-ray scattering contributed more anomalous features in the boson-peak regime [30]. In particular the group velocity of longitudinal sound (dispersion of the Brillouin line position) was found to exhibit a minimum at the wavenumber corresponding to the boson peak, and the sound attenuation (width of the Brillouin line) was found to increase strongly with frequency in the boson-peak regime (Rayleigh scattering) [31–36]. These anomalies were confirmed in computer simulations [37, 38]. We call all these features the boson-peak related anomalies.

The theoretical interpretation of the boson peak has a very diverse history and gave rise to several controversies [3]. In one line of argumentation for explaining the boson-peak related anomalies the authors tried to find a clas-

sical analogon of the tunneling model, the soft-potential model [39–41]. The bistable configurations, which can be described by an anharmonic double-well potential with a rather shallow barrier between the wells, were assumed to have a distribution of their characteristic parameters, in particular the second-order coefficient. It was found that in general the statistics of the vibrational excitations of such defect potentials would give rise to a constant density of eigenvalues $g(\omega^2)$, which leads to a DOS $g(\omega) \propto \omega$. On the other hand, so the argument, at lower frequencies (below a cross-over frequency ω_c) the balance between unstable configurations with negative second-order coefficients and the anharmonic fourth-order ones give rise to a defect DOS $\propto \omega^4$. Therefore the reduced DOS $g(\omega)/\omega$ increases $\propto \omega^2$ below ω_c and decreases $\propto \omega^{-1}$ above ω_c. In between, i.e. near ω_c is then the boson peak [39, 42].

Arguments that the boson peak, by its temperature characteristics, is not an anharmonic phenomenon were met by the authors of the soft-potential model by noting that the anharmonic interaction only acts in producing the soft configurations in the quenching process [43]. In the quenched state they are supposed to act like local harmonic oscillators, similar to heavy-mass atoms, coupled to the acoustic harmonic degrees of freedom [44–47].

Another attempt to explain the boson-peak anomaly was the phonon-fracton model [48–52]. It was postulated that disordered solids exhibit a certain degree of fractal structure. A fractal is a self-similar structure [53, 54], which has a non-integer dimensionality D_0, which is smaller than the embedding dimensionality d. Real fractals like sponges or trees have a smallest and largest scale, in which the self-similarity holds. The smallest scale is e.g. the smallest pore diameter of a sponge, the largest is the correlation length ξ. For scales larger than ξ the object looks like an ordinary material in which the mass scales as L^d, where L is the size. For scales smaller than ξ the mass scales as L^{D_0}. Alexander and Orbach [48] have shown that the vibrational degrees of freedom scale with a fractal dimensionality $d_s < D_0$ (spectral dimensionality) and that the DOS of such an object obeyes a Debye law below $\omega_\xi = 2\pi v/\xi$, where v is the sound velocity. Above ω_ξ the DOS behaves as $g(\omega) \propto \omega^{d_s-1}$. They found that in all fractal structures they investigated $d_s \approx 4/3$. The specific model employed by the phonon-fracton supporters was a percolating lattice, i.e. a cubic lattice in which a certain percentage of bonds $1-p$ (carrying neares-neighbor force constants) was missing. If the bond concentration p is larger than the critical concentration p_c, which determines the connectedness of the structure a finite correlation length $\xi \propto (p-p_c)^\nu$ exists (ν is the order-parameter exponent [52]). Calculations using the coherent-potential approximation (CPA) [55–57] showed that in between the Debye and the fracton regime an enhancement over the Debye $g(\omega) \propto \omega^2$ law was present [49, 50]. This was, for the time being, a satisfactory explanation of the boson peak. However, numerical simulations of the percolation-phonon-fracton model [52] showed that the phonon-fracton crossover in the DOS of this model occurs very smooth without any excess over the Debye law. Obviously the excess in the calculations [49, 50] had been an artifact of the CPA. Another argument against the phonon-fracton model as candidate for explaining the boson-peak anomalies is that - apart from aerogels [58, 59] glasses do not show any self-similary, which should show up (but does not) as an enhanced small-angle scattering in neutron or X-ray diffraction data.

In other articles reflecting on the vibrational anomalies of glasses the boson peak and the anomalous shoulder in the temperature dependence of the thermal conductivity were also considered to be related to Anderson localization of sound [51, 60, 61]. It was observed that near the boson-peak frequency the mean-free path of the acoustic excitations is of the order of the sound wavelength. According to a rule, coined by Ioffe and Regel in their survey of electronic conduction in semiconductors [62], the notion of a mean-free path, which implies a wave, which is occasionally scattered by an inhomogeneity, breaks down once the mean-free path becomes equal to the wavelength (Ioffe-Regel limit). Mott [63] conjectured that Anderson localization occurs for electrons near the Ioffe-Regel energy. For phonon it was assumed [61, 64], that the crossover from extended to Anderson-localized states would take place near the Ioffe-Regel frequency and that the boson peak would mark the onset of localized states. In particular it was thought, that the presence of localized states would cause the dip in the thermal conductivity [61]. Later, more detailed theoretical investigations showed, however, that the Anderson transition in realistic solids does not occur near the Ioffe-Regel crossover, but in a much higher frequency range near the Debye frequency [65–71].

Later many researchers were intested in whether the boson-peak frequency coincides exactly with the Ioffe-Regel frequency, given by the implicit relation $\omega_{IR} = \pi\Gamma(\omega_{IR})$, where $\Gamma(\omega)$ is the sound attenuation coefficient [72, 73]. $\Gamma(\omega)$ and hence ω_{IR} is, of course, different for longitudinal and transverse sound waves. It appeared that in materials governed by hard-sphere-like potentials the boson-peak coincides with the transverse Ioffe-Regel frequency [38, 74], whereas in network glasses with the longitudinal one [75–78].

In 1991 Schirmacher and Wagener [79] exploited the mathematical analogy between a single-particle random walk and harmonic phonons [80] using an off-lattice version of the CPA. They demonstrated that the cross-over from a frequency-independent conductivity/diffusivity to a frequency-dependent one [81, 82] corresponds to the onset of the frequency dependence of the complex sound velocity. The latter was found to lead to a boson peak in the vibrational DOS.

Because understanding this analogy is essential for grasping the essence of the BP-related anomalies, we devote a whole section of the present review to this analogy.

However, because the CPA in the case of the percolating lattice predicted a boson peak [49, 50], which did not exist in the simulation of the same system [52] a check was needed, whether the resulting boson-peak enhancement of the DOS was not an artifact of the CPA like in the phonon-fracton model. Therefore in Ref. [68] the lattice version of the CPA [83–85] was compared to a numerical calculation for a cubic lattice with fluctuating nearest-

neighbor force constants. Both simulation and CPA calculation showed a boson peak, and good agreement between CPA and the numerical spectrum was found. So it was demonstrated that effective-medium calculations are reliable for investigating the influence of disorder on the harmonic spectrum of a model solid. The breakdown of the CPA in the case of the phonon-fracton model was obviously due to the critical fluctuations in this model, which are not generic for disordered solids.

The boson peak in the model calculations of Ref. [68] was identified to be caused by very small positive and negative force constants, and being a precursor of an instability, which happens for stronger disorder [69, 70].

With the help of the numerical calculation in Ref. [68] it could also decided, whether the vibrational states near and above the boson peak were localized or extended. This was achieved by means of the statistics of the distances between the eigenvalues. Near and above the boson peak they showed the so-called Gaussian-ortogonal-ensemble (GOE) statistics of random-matrix theory [86, 87], which proves that the corresponding states are delocalized. At high frequencies, near the upper band edghe a transition to Poissonian statistics was observed, which is evidence for a delocalization-localization transition in this regime, in agreement with earlier estimates [65, 66]. On the other hand, the GOE statistics is a sign for the so-called level repulsion, showing that each eigenvalue is non-degenerate due to the absence of symmetries in the disordered system. As the generic spectrum of random matrices is not a Debye spectrum (which is highly degenerate) the boson peak marks the transition from a Debye to a random-matrix-type spectrum [6].

The spectra calculated in Ref. [68] for a cubic lattice with very small disorder exhibited the usual van-Hove singularities, which appear as a result of the leveling-off of the crystalline phonon dispersions $\omega(k)$ at the Brillouin-zone boundary [88]. With increasing disorder the data showed that the sharp van-Hove peak became rounder and is shifted downwards and gradually transformed to the low-frequency boson peak. This led Taraskin et al. [89] to the conclusion that the boson peak is just a crystal-like van-Hove peak, modified by disorder. This appeared as a rather unexpected conclusion, because a van-Hove singularity is a typical signature of a crystalline structure with long-range order and was not known to exist in glasses. However, until now, the boson peak explanation as a glassy version of a van-Hove singularity is still considered to be an alternative to the disorder explanation [90–92]. We further comment on this in section IV.

Quite recently in an experimental study of a macroscopic disordered model glass it was shown that the disorder-induced maximum of the reduced DOS and that induced by the van-Hove mechanism are, in fact, two different phenomena [93].

The random-matrix aspect of the disorder-vibration problem was elaborated further in the literature [94–104], in particular by means of the euclidean random-matrix theory [96–103].

As in Ref. [68] a disorder-induced boson peak was found and shown to be the precursor of an instability ("phonon-saddle transition" [100]).

A quite different and interesting approach to the boson-peak anomaly was worked out [105] in the framework of the mode-coupling theory of the glass transition . This theory of glassy freezing in its original form [106, 107] describes the idealized glass transition as a dynamical transition towards a non-ergodic state leading to a frozen-in additional contribution to the static longitudinal susceptibility. This, in turn leads to a characteristic hump in the density fluctuation spectrum of the idealized glass (proportional to the neuton scattering law $S(k,\omega)$), which was identified with the boson-peak anomaly found in neutron scattering experiments. Interestingly this theory already predicted the characteristic dip in the longitudinal group velocity, which was found later to be associated with the boson peak, as mentioned above [31, 35, 37, 38].

We feel that an important step in the understanding of the boson peak was achieved by working out heterogeneous-elasticity theory [22]. In this phenomenological theory it is assumed that the shear modulus in ordinary elasticity theory [108] is assumed to exhibit spatial fluctuations. The resulting stochastic equations were solved by field-theoretical techniques [65, 109], resulting in a mean-field theory, called self-consistent Born approximation (SCBA). The SCBA is obtained from assuming a Gaussian distribution of the elasticity fluctuations and that the relative width of the Gaussian is a small parameter ("disorder parameter" γ). Again, if the disorder parameter becomes larger than a critical one, an instability occurs, which is due to too many regions with negative elastic constants.

Shortly before heterogeneous-elasticity theory had been worked out a series of papers appeared, in which molecular-dynamics simulations of glasses were investigated for their elastic and vibrational properties [110–113]. It turned out that, by applying external forces, indeed heterogeneous shear deformations are present. The authors showed that in regions with strong deformations the shear response is highly non-affine, i.e. the displacements do not follow the direction of the applied stress. In the non-affine regions the local shear moduli were found to be very small and even negative, a finding, which was observed also in other simulations [38, 114, 115]. This nicely confirmed the model assumption of heterogeneous-elasticith theory. In Ref. [38] a direct comparison between the elasticity fluctuations in a simulated glass and the theory of Ref. [22] was made and good agreement was found. We shall comment on this article in more detail below.

The non-affine character of disordered elasticity has been described from a fundamental theoretical basis recently [116] and, very recently, shown to be an important ingredient for a disorder characterization of glasses /citepan21

An important aspect of the boson peak appeared when it was shown [117] with the help of heterogeneous-elasticity theory that the excess DOS $\Delta g(\omega) = g(\omega) - g_D(\omega)$ with respect to the Debye DOS $g_D(\omega)$ is proportional to the sound attenuation in the boson-peak

frequency range. Heterogeneous-elasticity provides an expression for the disorder-induced sound attenuation as imaginary part of frequency-dependent elastic coefficients (see section ..). These enter into the spectral functions, and the DOS enhancement is just produced by the sound attenuation, which increases rapidly in the boson-peak frequency regime due to Rayleigh scattering.

The rest of this contribution is organized as follows: In section II. the mathematical analogy between diffusion and scalar elasticity is investigated in detail and two mean-field or effective-medium theories, the self-consistent Born approximation (SCBA) and the coherent-potential approximation (CPA) for this model are introduced and solved. A pedagogical derivation, which is more simple than the original field-theoretical one, is presented. We show that the boson-peak related anomalies are the analogon of the crossover from a frequency-independent diffusivity/conductivity to a frequency-dependent one.

In section III. the full vectorial heterogeneous elasticity theory is presented and solved in SCBA and CPA. The salient features of the boson-peak related anomalies of glasses are discussed with the help of these mean-field theories. In section IV. we discuss recent conflicting theories of these anomalies.

II. "SCALAR ELASTICITY" AND DIFFUSION-VIBRATION ANALOGY

A. Diffusion-vibration analogy

A simplified version of heterogeneous elasticity theory, which proved to be helpful in understanding the spectral properties of disordered solids [46, 79, 100, 118–120] is represented by a scalar wave equation with a spatially fluctuating elastic constant $K(\mathbf{r}) \equiv \rho\widetilde{K}(\mathbf{r})$ (ρ is the mass density)

$$\frac{\partial^2}{\partial t^2}u(\mathbf{r},t) = \nabla\widetilde{K}(\mathbf{r})\nabla u(\mathbf{r},t) \tag{1}$$

The elastic coefficient $\widetilde{K}(\mathbf{r})$, which is the square of the local sound velocity, $v(\mathbf{r})$ may be sub-divided into an average elasticity $\widetilde{K}_0 = \langle\widetilde{K}\rangle$ and deviations $\Delta\widetilde{K}(\mathbf{r})$

$$\widetilde{K}(\mathbf{r}) = v^2(\mathbf{r}) = \widetilde{K}_0 + \Delta\widetilde{K}(\mathbf{r}) \tag{2}$$

If we replace the second time derivative in Eq. (1) by a first one, we arrive at a diffusion equation, which describes the random walk of a particle, which encounters a spatially varying diffusivity, e.g. due to a spatially varying activation energy

$$\begin{aligned}\frac{\partial}{\partial t}n(\mathbf{r},t) &= \nabla D(\mathbf{r})\nabla n(\mathbf{r},t)\\ &= \nabla\Big[D_0 + \Delta D(\mathbf{r})\Big]\nabla n(\mathbf{r},t)\end{aligned} \tag{3}$$

with D_0, again, denoting the avarage diffusivity and $\Delta D(\mathbf{r})$ the fluctations. $n(\mathbf{r},t)$ is the probability density for finding the particle within a volume element around $\mathbf{r}$ at time t. The Green's function of Eq. (1) in frequency space obeys the equation

$$\begin{aligned}&\Big(-z^2 - \nabla\widetilde{K}(\mathbf{r})\nabla\Big)G(\mathbf{r},\mathbf{r}')\\ =\ &\Big(-z^2 - \nabla\big[\widetilde{K}_0 + \Delta\widetilde{K}(\mathbf{r})\big]\nabla\Big)G(\mathbf{r},\mathbf{r}')\\ \equiv\ & A[z,\mathbf{r},\widetilde{K}(\mathbf{r})]G(\mathbf{r},\mathbf{r}') = \delta(\mathbf{r}-\mathbf{r}')\end{aligned} \tag{4}$$

with $z = \omega + i\epsilon, \epsilon \to +0$. The operator $A[z,\mathbf{r},\widetilde{K}(\mathbf{r})]$ is the operator-inverse of the Green's function. On the other hand the Green's function corresponding to the heterogeneous diffusion equation (3) in frequency space is

$$s - \nabla D(\mathbf{r})\nabla G(\mathbf{r},\mathbf{r}') = \delta(\mathbf{r}-\mathbf{r}') \tag{5}$$

with $s = i\omega + \epsilon$.

So all calculations done for the scalar vibration problem (4) can be taken over for the diffusion problem (5) provided we identify $D \leftrightarrow \widetilde{K}$, $s \leftrightarrow -z^2$, or $i\omega \leftrightarrow -\omega^2$.

In the next three subsection we shall demonstrate by means of different approximation schemes (Born approx, Self-consistent Born approx. and coherent-potential approx.) that the quenched glassy disorder induces a characteristic frequency dependence to the macroscopic diffusivity/elasticity. So these approximation schemes act as a coarse-graining scheme, which converts spatial fluctuations to frequency dependences.

In this context we may distinguish between three characteristic scales: the microscopic scale, the mesoscopic scale and the macroscopic one. The microscopic scale is the molecular one and may be described by microscopic quantum or classical equations of motions. The mesoscopic scale is a scale of 5 or 6 atomic or molecular diameter. This is the minimal scale at which one may define local diffusivities or elastic constants [38, 114, 115, 120, 121], which exhibit spatial fluctuations in structurally disordered materials. The macroscopic scale is the experimental one (mm or cm), in which the macroscopic diffusivities or elastic coefficients are frequency-dependent.

B. Low frequency limit: Born approximation, Rayleigh scattering and long-time tails

The solution of Eq. (4) or (5) without fluctuations is given in $\mathbf{k}$ space by ($\mathbf{k}$ is the wave vector corresponding to $\mathbf{r}-\mathbf{r}' \equiv \tilde{\mathbf{r}}$)

$$G_0(k,z) = \frac{1}{-z^2 + \widetilde{K}_0 k^2} \tag{6}$$

The disorder-averaged full Green's function should also only depend on $|\tilde{\mathbf{r}}|$ only and therefore may be represented as [119]

$$\begin{aligned}\langle G(z)\rangle_{\mathbf{k}} &= \mathsf{G}(\mathbf{k},z) = \frac{1}{-z^2 + k^2(\widetilde{K}_0 - \Sigma(z))}\\ &\equiv \frac{1}{-z^2 + k^2 Q(z)}\end{aligned} \tag{7}$$

where $\Sigma(z) = \Sigma'(\omega) + i\Sigma''(\omega)$ is the self-energy function, which describes the influence of the fluctuations $\Delta\widetilde{K}(\mathbf{r})$ or $\Delta D(\mathbf{r})$. Here we have defined a frequency-dependent elasticity $Q(z) = \widetilde{K}_0 - \Sigma(z)$, corresponding to a frequency-dependent diffusivity $D(s) = D_0 - \Sigma(s)$. The former may be identified with the square of a frequency-dependent sound velocity $v(z)$, i.e. $Q(z) = v(z)^2$.

To lowest order in the fluctuations one obtains by straightforward perturbation theory [119] the Born approximation

$$\Sigma(z) = \gamma \frac{1}{V} \sum_{\mathbf{k}} k^2 G_0(\mathbf{k}, z)\,, \tag{8}$$

where $\sum_{\mathbf{k}} \equiv \frac{V}{(2\pi)^3} \int d^3\mathbf{k}$, V is the sample volume, and

$$\gamma = \langle \Delta\widetilde{K}^2 \rangle V_c\,, \tag{9}$$

i.e. the variance of $\widetilde{K}(\mathbf{r})$ times a coarse-graining volume V_c, which serves to calculate the local elastic coefficient [38, 119, 121].

If one imposes an upper cutoff $k_{\max}$ in the wavenumber integration, the integral in Eq. (8) can be done exactly. For small frequencies we obtain

$$\Delta\Sigma(s) = \Sigma(z) - \Sigma(0) \propto s^{3/2} \tag{10}$$

For the vibrational problem $s^{3/2} \to i\omega^3$.

We now show that this leads to Rayleigh's ω^4 scattering law [122, 123]:

We may be interested in the wave intensity given by the modulus of Eq. (7)

$$|G(\tilde{\mathbf{r}}, z)|^2 = \left(\frac{1}{4\pi\widetilde{K}_0}\right)^2 e^{-\tilde{r}/\ell(\omega)} \tag{11}$$

with the mean-free path

$$\begin{aligned} \frac{1}{\ell(\omega)} &= 2\mathrm{Im}\Big\{\frac{\omega}{v(\omega)}\Big\} \\ &\approx \frac{\Sigma''(\omega)\omega}{v_0^3} = \frac{\gamma}{12\pi}\left(\frac{\omega}{v_0}\right)^4 \end{aligned} \tag{12}$$

where $v_0 = \sqrt{\widetilde{K}_0}$.

Eq. (12) constitutes the *Rayleigh scattering law* [122, 123]. It holds for harmonic excitations in the presence of quenched disorder [103, 119], provided the disorder fluctuations do not exhibit long-range order [119, 124, 125].

Rayleigh scattering in Glasses is usually obscured by anharmonic sound attenuation, which prevails in the sub-THz frequency range. It has been observed experimentally in the THz regime in some glasses [31, 35] as well in computer simulations [37, 38].

In the diffusion problem $D(s)$ is the frequency-dependent diffusivity, which can be shown [126] to be the Laplace transform of the velocity autocorrelation function $Z(t)$ of the moving particle $D(s) = \int_0^\infty dt e^{-st} Z(t)$

We apply the Tauberian theorem [127]

$$\lim_{s\to 0} D(s) \propto s^{-\rho} \quad \Leftrightarrow \quad \lim_{t\to\infty} D(t) \propto t^{\rho-1} \tag{13}$$

from which we conclude

$$\lim_{t\to\infty} Z(t) \propto t^{-5/2}\,, \tag{14}$$

a behaviour well known for particles performing a random walk in a quenched-disordered environment [128, 129].

On the other hand, by the Nernst-Einstein relation

$$\sigma(s) = \sigma'(\omega) + i\sigma''(\omega) = \frac{ne^2}{k_B T} \tag{15}$$

the frequency-dependent diffusivity is related to the dynamic conductivity, the real part of which, $\sigma'(\omega)$ is the alternate-current (AC) conductivity. Therefore, one expects a non-analytic low-frequency dependence of the AC conductivity increment $\sigma'(\omega) - \sigma(0) \propto \omega^{3/2}$. Indeed, such a behavior has been observed in amorphous semiconductors [130]. We come back to this in the subsection on strong disorder.

C. Weak disorder and the self-consistent Born approximation (SCBA)

A well-known characteristic of the AC conductivity in disordered materials is that beyond a characteristic frequency ω^* it starts to increase with frequency, in many cases with a characteristic power law $\sigma'(\omega) \propto \omega^\alpha$ where α is smaller than 1 and takes values around 0.8 [81, 82, 131].

For the random walker in the disordered environment this means that the mean-square distance walked does not increase linearly with time but sublinearly with exponent $1 - \alpha$. Such a behavior has been termed anomalous diffusion. So the cross-over at ω^* corresponds to a transition from anomalous diffusion for times $t < 1/\omega^*$ to normal diffusion for $t > 1/\omega^*$.

As pointed out in Refs. [79, 120] the cross-over at ω^* - if transformed from the diffusion to the scalar-vibrational system - corresponds to the boson peak. In other words: it correspondss to the begin of the frequency dependence of $\widetilde{K}(\omega) = v(\omega^2)$. By the Kramers-Kronig correspondence this implies the onset of an imaginary part of $\widetilde{K}(\omega)$ which becomes of the order of its real part.

A minimal theory for the boson peak, in fact, can be obtained by the *self-consistent* version of the Born approxmation. It is obtained by replacing the bare Green's function in Eq. (8) by the full Green's function:

$$\Sigma(z) = \gamma \frac{1}{V} \sum_{|\mathbf{k}| \le k_{\max}} k^2 \mathsf{G}(\mathbf{k}, z) \tag{16}$$

with $\mathsf{G}(k, z)$ given by Eq. (7). For the ultraviolet cutoff $k_{\max}$ one should take the inverse of the length scale which is the diameter of the coarse-graining volume V_c used to define the local elastic constant/local diffusivity [119]. On the other hand this length scale should be of the order of the correlation length ξ of the elasticity/diffusivity fluctuations [124]. In this work we treat these two length scale as being the same. We therefore call the cutoff $k_{\max} = k_\xi$.

While the "derivation" of Eq. (16) is, of course, just an ad-hoc replacement, a proper derivation is achieved by field-theoretical techniques [46] in analogy to the derivation of the nonlinear sigma model for electrons [109, 132–134], classical sound waves [65, 124] and electromagnetic waves [135, 136].

A royal road for this derivation is to minimize the following (dimensionless, frequency-dependent) mean-field free energy or effective action with respect to $\Sigma(z)$

$$S_{\rm eff}[\Sigma(z)] = S_{\rm med}[\Sigma(z)] + S_{\rm SCBA}[\Sigma(z)] \tag{17}$$

with

$$\begin{aligned} &S_{\rm med}[\Sigma(z)] = S_{\rm med}[Q(z)] \\ &= {\rm Tr}\ln\Big(A\big[z,\mathbf{r},\underbrace{\widetilde{K}_0-\Sigma(z)}_{Q(z)}\big]\Big) = \sum_{\mathbf{k}}\ln\Big(A\big[z,\mathbf{k},Q(z)\big]\Big) \end{aligned} \tag{18}$$

and

$$S_{\rm SCBA}[\Sigma(z)] = \frac{1}{2}\frac{V}{\gamma}\Sigma(z)^2 \tag{19}$$

The first term, $S_{\rm med}[\Sigma(z)]$, is the generalized free energy of the effective medium [137], which is a medium without disorder, in which the fluctuating force constants in the operator $A[z,\mathbf{r},\widetilde{K}(\mathbf{r})]$ are replaced by the homogeneous (but frequency-dependent) force constant $Q(z) = K_0 - \Sigma(z)$. The trace can therefore be calculated in $\mathbf{k}$ space. The Fourier transform of $A[z,\mathbf{r},Q(z)]$ is given by

$$A[z,\mathbf{k},Q(z)] = -z^2 + k^2 Q(z) \tag{20}$$

This is no more the operator-inverse but just the ordinary inverse of the mean-field Green's function

$$\begin{aligned} G(\mathbf{k},z) &= \frac{1}{A[z,\mathbf{k},Q(z)]} \\ &= \frac{1}{-z^2+k^2Q(z)} \end{aligned} \tag{21}$$

The second term, $S_{\rm SCBA}[\Sigma(z)]$ arises [22, 65] from a Gaussian configuration average of the full Green's function with distribution density

$$P\big[\Delta\widetilde{K}(\mathbf{r})\big] = P_0\exp\{-\frac{1}{2\gamma}\int d^3\mathbf{r}[\Delta\widetilde{K}(\mathbf{r})]^2\} \tag{22}$$

It is easily verified that the SCBA (16) is obtained by minimizing $S_{\rm eff}$ of Eq. (18). This corresponds to the saddle-point approximation of the effective field theory derived for the appropriate stochastic Helmholtz equation [22, 65, 109, 118]. The saddle-point approximation relies on the large prefactor of $S_{SCBA} \propto 1/\gamma$, i.e. the SCBA has its validity range for

(i) small disorder $\langle K^2\rangle/K_0^2 \ll 1$;

(ii) Gaussian disorder, Eq. (22).

As in our calculation of the Rayleigh scattering and the non-analyticity of $D(s)$ the SCBA transforms the microscopic wave equation with fluctuating elastic coefficient

$$\big[-z^2 - \nabla\widetilde{K}(\mathbf{r})\nabla\big]u(\mathbf{r},z) \tag{23}$$

into a macroscopic mean-field wave equation

$$\big[-z^2 - \widetilde{K}(z)\nabla^2\big]u(\mathbf{r},z) \tag{24}$$

The fluctuations of $\widetilde{K}(\mathbf{r})$, (represented by the variance) determine the frequency dependence of $\widetilde{K}(z)$.

It is useful to formulate the SCBA, Eq. (16) in dimensionless units (indicated by a hat). We measure velocities in units of $\sqrt{\widetilde{K}_0}$, lengths in units of k_ξ, and angular frequencies in units of $k_\xi\sqrt{\widetilde{K}_0}$. (In the diffusion problem diffusivities are measured in units of D_0 and angular frequencies in units of $D_0k_\xi^2$.) In these units the SCBA, Eq. (16) takes the form

$$\widehat{\Sigma}(\hat{z}) = \frac{\Sigma(z)}{\widetilde{K}_0} = 3\widehat{\gamma}\int_0^1 d\hat{k}\hat{k}^2\frac{\hat{k}^2}{-\hat{z}^2+\hat{k}^2[1-\widehat{\Sigma}(\hat{z})]} \tag{25}$$

with the dimensionless "disorder parameter"

$$\widehat{\gamma} = \gamma\frac{\nu}{\widetilde{K}_0^2} = V_c\nu\frac{\langle(\Delta\widetilde{K})^2\rangle}{\widetilde{K}_0^2} \tag{26}$$

For $\hat{z}=0$ Eq. (25) takes the form

$$\widehat{\Sigma}(0) = \frac{\widehat{\gamma}}{1-\widehat{\Sigma}(0} \tag{27}$$

This quadratic equation has the solution

$$\widehat{\Sigma}(0) = \frac{1}{2}\Big[-1+\sqrt{1-4\widehat{\gamma}}\Big] \tag{28}$$

We observe that for $\widehat{\gamma} > \widehat{\gamma}_c = 1/4$ no real solution is obtained. This indicates an instability, i.e. for $\widehat{\gamma} > \widehat{\gamma}_c$ the SCBA predicts eigenvalues $\omega^<0$. This can be rationalized by the fact that the SCBA is obtained from assuming a Gaussian distribution (22). If the width of this distribution exceed a critical value, there exist too many local regions with negative elastic coefficients, which then leads to the instability. Within this model a strong boson peak is obtained if the disorder parameter $\widehat{\gamma}$ approaches the critical value $\widehat{\gamma}_c$.

If we assume that the Debye cutoff $k_D = \sqrt[3]{6\pi^2N/V}$ coincides with k_ξ (N is the number of atoms or molecular units and V the sample volume), the density of states is given by

$$g(\hat{\omega}) = \frac{2\hat{\omega}}{\pi}3\int_0^1 d\hat{k}\hat{k}^2{\rm Im}\left\{\frac{1}{-\hat{z}^2+k^2\big[1-\widehat{\Sigma}(\hat{z})\big]}\right\} \tag{29}$$

In Fig. 1 we have plotted the frequency-dependent diffusivity (panel a) together with the DOS, divided by the Debye DOS $g_D\hat{\omega} = 3\hat{\omega}^2/\hat{\omega}_D^3$ (reduced DOS), with $\hat{\omega}_D = \sqrt{1-\widehat{\Sigma}_0}$, for different values of $\widehat{\gamma}$ near $\widehat{\gamma}_c$. We see that the boson peaks indeed coincide with the onset of the frequency dependence of $D(\omega)$.

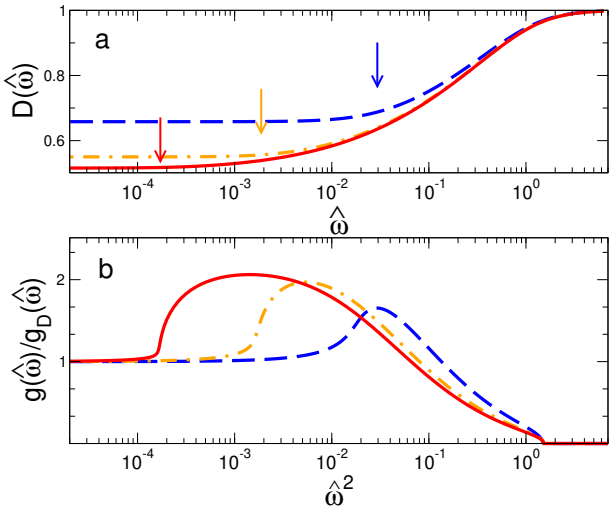

FIG. 1. Panel a: Frequency-dependent diffusivity, calculated in SCBA, Eq. (25) with disorder parameters $(\hat{\gamma}-\hat{\gamma}_c)/\hat{\gamma}_c = 10^{-1}$ (blue dashes), 10^{-2} (orange dash-dots), 10^{-3} (red line). Panel b: Reduced density of states $g(\omega)/g_D(\omega)$ for the same parameters as in panel a and setting $k^\xi = k_D$.

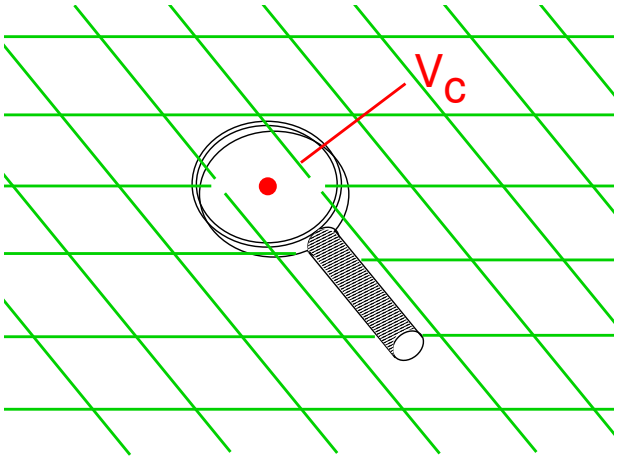

FIG. 2. Visualization of the continuum version of the CPA: Inside a volume V_c of the effective medium with homogeneous elasticity $Q(z)$ the homogeneous one is replaced by the fluctuating one $\widetilde{K}(\mathbf{r})$, which gives rise to a perturbation $\widetilde{K}(\mathbf{r})-Q(z)$. The CPA postulate is to minimize the influence of this perturbation, i.e. forcing the averaged T matrix of the perturbation to be equal to zero.

D. Strong disorder and the coherent-potential approximation (CPA)

It is clear from Fig. 1 that the frequency dependence of the diffusivity (and hence of the AC conductivity), predicted by the SCBA is rather weak, as compared to the strong frequency dependence of the conductivity in ionic conducting glasses or amorphous semiconductors [81, 82]. This is so, because the SCBA is restricted to very weak disorder. In materials with activated ionic or electronic hopping conduction, on the other hand, the local diffusivities fluctuate very strongly, because they depend exponentially on local activation energies and local tunneling distances [138, 139].

A rather successful and reliable mean-field theory for strong disorder is the coherent-potential approximation (CPA). It was widely used for electronic structure calculations of disordered crystals [140–142], and later to diffusion and vibrational properties of disordered crystals [68, 83–85, 89]. In this lattice version of the CPA one consider a certain lattice site of the ordered effective medium, in which the potentials [140–142], the force constants or the diffusivities [68, 83–85, 89] are homogeneous ("coherent") but frequency-dependent. At this special site the effective medium is replaced by the real medium, causing a "perturbation" of the effective medium. Enforcing now the averaged T matrix of this perturbation to vanish gives the self-consistent CPA equation for the coherent potential.

A version suitable for non-crystalline materials has been worked out by S. Köhler and the present authors using field-theoretical techniques. [120]. The resulting CPA equation may be pedagogically visualized in the following way, see Fig. 2: in a certain region of the effective medium the frequency-dependent elasticity $Q(z)$ is replaced by the fluctuating one $\widetilde{K}(\mathbf{r}_i)$, where $\mathbf{r}_i$ is the mid-point of the region. The CPA postulate takes the form

$$\left\langle \frac{\widetilde{K}(\mathbf{r}_i)-Q(z)}{1+\Lambda(z)[\widetilde{K}(\mathbf{r}_i)-Q(z)]} \right\rangle = 0 \tag{30}$$

The average is over the distribution of the elasticity values $\widetilde{K}(\mathbf{r}_i) \equiv \widetilde{K}_i$ with distribution density $P(\widetilde{K}_i)$. The latter may be taylored to the statistics of the disordered material at hand.

$\Lambda(z)$ generalizes the effective-medium propagator in the lattice CPA. Both $\Lambda(z)$ and $Q(z)$ may be obtained by minimizing the following mean-field action

$$S_{\rm eff}[Q(z),\Lambda(z)] = S_{\rm med}[Q(z)] + S_{\rm CPA}[Q(z),\Lambda(z)] \tag{31}$$

where $S_{\rm med}[Q(z)]$ is given by Eq. (18) and the CPA action by

$$S_{CPA}[Q(z),\Lambda(z)] = \frac{V}{V_c}\left\langle \ln\left(1+\Lambda(z)[\widetilde{K}(\mathbf{r}_i)-Q(z)]\right)\right\rangle \tag{32}$$

The large parameter of the saddle-point approximation, which validates the mean-field approximation, is now *not* the inverse disorder parameter, as in the case of the SCBA, but the parameter V/V_c. This is the reason, why the CPA is not restricted to small disorder. Varying the action with respect to $\Lambda(z)$ we obtain the CPA equation (30), which can be put into the equivalent forms

$$\left\langle \frac{1}{1+\Lambda(z)[\widetilde{K}_i-Q(z)]} \right\rangle = 1 \tag{33}$$

$$Q(z) = \left\langle \frac{\widetilde{K}_i}{1+\Lambda(z)[\widetilde{K}_i-Q(z)]} \right\rangle . \tag{34}$$

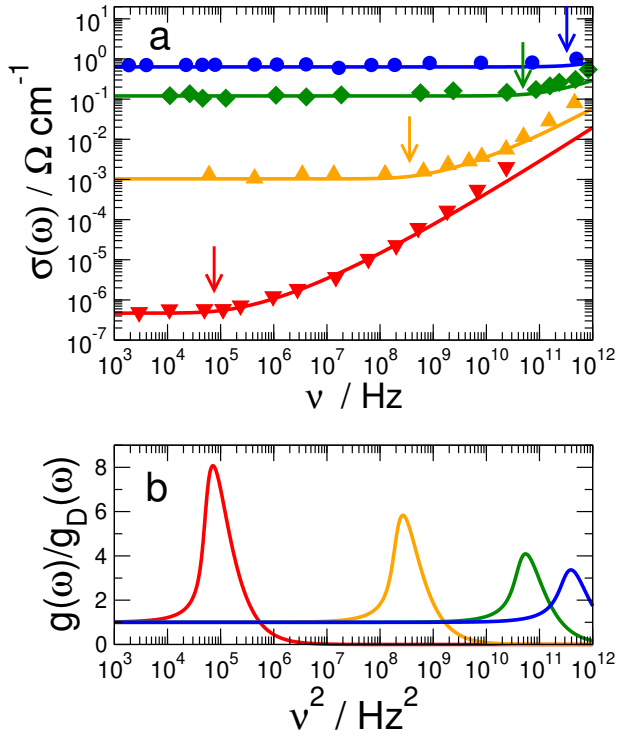

FIG. 3. Panel a: Full lines: Frequency-dependent diffusivity, calculated in CPA, Eq. (74), with a flat distribution of activation energies, Eq. (41). Symbols: AC conductivity data of the ionic-conducting glass Sodium Trisilicate, compiled by Wong and Angell [143]. with disorder parameters $\widetilde{\gamma} = 7.92$ ($\leftrightarrow T = 1673$ K); $= 10.41$ ($\leftrightarrow T = 1273$ K); $= 17.53$ ($\leftrightarrow T = 756$ K); $= 29.06$ ($\leftrightarrow T = 456$ K); (from top to bottom).

Panel b: Reduced density of states $g(\hat{\omega})/g_D(\hat{\omega})$ for the equivalent distribution density (42) for the same parameters as in panel a.

Varying the action with respect to $Q(z)$ gives a relation for $\Lambda(z)$:

$$\sum_{\mathbf{k}} \frac{k^2}{-z^2 + k^2 Q(z)} = \frac{V}{V_c}\Lambda(z) \left\langle \frac{1}{1 + \Lambda(z)[\widetilde{K}_i - Q(z)]} \right\rangle = \frac{V}{V_c}\Lambda(z)\,, \tag{35}$$

where the second line follows from Eq. (33).

It is advantageous to normalize the $\mathbf{k}$ integration to 1

$$\Lambda(z) = \frac{V_c}{V}\sum_{\mathbf{k}} \frac{k^2}{-z^2 + k^2 Q(z)} = p\chi^{\xi}(z) \tag{36}$$

with

$$\chi^{\xi}(z) = \frac{3}{k_\xi^3}\int_0^{k_\xi} dk k^2 \frac{k^2}{-z^2 + k^2 Q(z)} \tag{37}$$

and

$$p = \frac{V_c k_\xi^3}{6\pi^2} \tag{38}$$

p should be smaller than 1, and It has been argued in Ref. [120] that one may identify p with the continuum percolation concentration p_c. One has $\chi^{\xi}(z{=}0) = 1/Q(0)$.

The CPA equation (34) now takes the form

$$Q(z) = \left\langle \frac{\widetilde{K}_i}{1 + p\chi^{\xi}(z)[\widetilde{K}_i - Q(z)]} \right\rangle . \tag{39}$$

As in the case of the SCBA the CPA turns the wave equation with fluctuating elasticity into a mean-field wave equation with frequency-dependent elastic coefficient $Q(z)$ or a diffusion equation with frequency-dependent diffusivity $D(s)$.

Let us now identify $\widetilde{K}_i$ with a spatially fluctating diffusivity D_i and assume that the fluctations are caused by a fluctuating activation energy

$$D_i = D_0 e^{-E_i/k_B T} \tag{40}$$

If we now impose a constant distribution density of activation energies

$$P(E_i)\frac{1}{E_c}\theta(E_c - E_i) \tag{41}$$

i.e. a flat distribution with cutoff E_c. For the diffusivities D_i (or elasticities $\widetilde{K}_i$) this transforms to a truncated inverse-power distribution [**?**]

$$P(\widetilde{K}_i) = \frac{1}{\mu_1/\mu_2}\frac{1}{\widetilde{K}_i} \qquad \mu_1 \le \widetilde{K}_i \le \mu_2 \tag{42}$$

with $\mu_1 = \mu_2 e^{-E_c/k_B}$, and we have

$$\frac{1}{\langle\widetilde{K}\rangle^2}(\langle\widetilde{K}^2\rangle - \langle\widetilde{K}\rangle^2) = \frac{1}{2}E_c/k_B T \equiv \widetilde{\gamma} \tag{43}$$

Low temperatures in the diffusion problem obviously mean strong disorder.

In panel a of Fig. 3 we have plotted AC conductivity data for the glassy ionic conductor Sodium Trisilicate [143]. Together with these data we plot the CPA result with a distribution of activation energies as given in Eq. (41). In panel b of this figure we have plotted the reduced DOS of the equivalent vibrational problem with inverse-power distribution (42). The DOS for the scalar phonon problem is given by

$$g(\omega) = \frac{2\omega}{\pi}\mathrm{Im}\left\{\frac{1}{N}\sum_{|\mathbf{k}|\le k_D} \frac{1}{-z^2 + k^2 Q(z)}\right\} \tag{44}$$

Apart from the perfect agreement between the conductivity data and the CPA curves we note that the (rather strong) boson peak precisely mark the crossover from frequency-independent to frequency-dependent conductivity of the diffusion problem. In the vibrational problem this crossover means a transition from a regime with Debye waves and Rayleigh scattering to a non-Debye regime, in which the vibrational excitations are not waves. These excitations have been called "diffusons" [144], because their intensity obeys a diffusion equation like light in turbid media [145]. On the other hand, the vibrational excitations in this regime show the statistical properties of random matrices [68, 94, 104]. Therefore

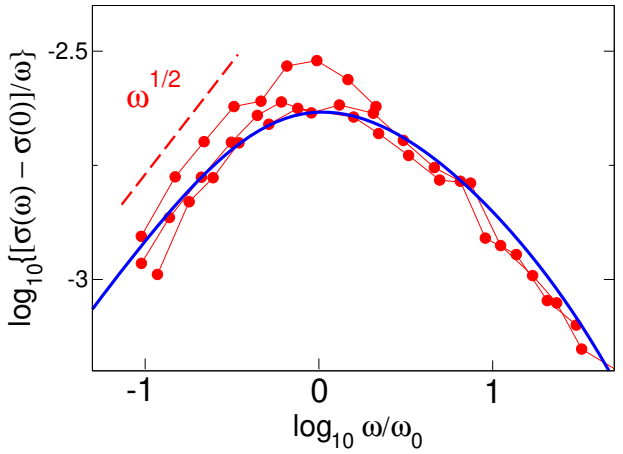

FIG. 4. Connected symbols: AC loss function $[\sigma(\omega)-\sigma(0)]/\omega$, measured in sputtered amorphous silicon [130] for three different temperatures (T = 51 K, 77 K, 154 K). The scaling frequency $\omega_0(T)$ is proportional to $\sigma(0,T)$. Full thick line: CPA calculation for a constant distribution of activation energies.

the frequency regime above the boson peak may also be called "random-matrix regime" [6, 7].

Returning to the diffusion problem, we pointed out that in the frequency range below the crossover (the frequency-independent regime) the Rayleigh scattering corresponds to a contribution to the frequency dependent conductivity with $\Delta\sigma'(\omega) \propto \omega^{3/2}$. This may be experimentally verified by considering the dielectric loss function

$$\epsilon''(\omega) \propto \frac{1}{\omega}\big[\sigma'(\omega) - \sigma(0)\big] \tag{45}$$

In the frequency-independent regime this function *increases* with frequency $\epsilon'' \propto \omega^{1/2}$, whereas in the frequency-dependent regime it *decreases* due to the sublinear behavior of $\sigma'(\omega)$. The maximum of the loss function corresponds to the maximum of the reduced DOS in the vibrational problem (boson peak).

It has been noted in the literature [131] that the AC conductivity data taken at different temperatures show universal behavior, if the data are divided by the DC conductivity $\sigma(0,T)$ and the freqency by the crossover frequency $\omega_0(T) \propto \sigma(0,T)$. For the loss function this means that $\epsilon''(\omega/\omega_0)$ should also be the same for different temperatures.

In Fig. 4 we show the loss function of sputtered amorphous silicon [130] against ω/ω_0 for three temperatures, together with the result of the CPA, which predict the scaling and the crossover from $\epsilon'' \propto \omega^{1/2}$ to the decrease with frequency. We discuss the corresponding scaling of the vibrational DOS in section III D.

III. HETEROGENEOUS-ELASTICITY THEORY

A. Model

We now formulate the full heterogeneous-elasticity theory for vector displacements $\mathbf{u}(\mathbf{r},t)$ The equation of motion for an elastic medium with spatially fluctuating shear modulus $G(\mathbf{r})$[1]

$$\big[\frac{\partial^2}{\partial t^2} - \nabla\cdot\widetilde{M}(\mathbf{r})\nabla\cdot\ + \nabla\times\widetilde{G}(\mathbf{r})\nabla\times\big]\mathbf{u}(\mathbf{r},\omega) = 0 \tag{46}$$

with the reduced shear modulus $\widetilde{G}(\mathbf{r}) = G(\mathbf{r})/\rho$ and the reduced longitudinal modulus

$$\widetilde{M}(\mathbf{r}) = M(\mathbf{r})/\rho = \widetilde{K} + \frac{4}{3}\widetilde{G}(\mathbf{r}) \tag{47}$$

In this formulation the dilatational (bulk) modulus $K = \widetilde{K}/\rho$ is assumed not to exhibit spatial fluctuations, i.e. the fluctuations of the shear modulus $G(\mathbf{r}) = \widetilde{G}(\mathbf{r})/\rho$ are assumed to affect the traceless stress and strain tensors only [7, 120].

Eqs. (46) may be decoupled by introducing longitudinal and transverse displacements $\mathbf{u}_L(\mathbf{r},t)$ and $\mathbf{u}_T(\mathbf{r},t)$ with

$$\nabla\times\mathbf{u}_L(\mathbf{r},t) = 0 \qquad \text{and} \qquad \nabla\cdot\mathbf{u}_T(\mathbf{r},t) = 0 \tag{48}$$

In the frequency domain we then have

$$\begin{aligned} 0 &= \Big(-z^2 - \nabla\cdot\widetilde{M}(\mathbf{r})\nabla\cdot\Big)\mathbf{u}_L(\mathbf{r},z) \\ &\equiv A_L[z,\mathbf{r},\widetilde{G}(\mathbf{r})]\mathbf{u}_L(\mathbf{r},z) \end{aligned} \tag{49}$$

$$\begin{aligned} 0 &= \Big(-z^2 + \nabla\times\widetilde{G}(\mathbf{r})\nabla\times\Big)\mathbf{u}_T(\mathbf{r},z) \\ &\equiv A_T[z,\mathbf{r},\widetilde{G}(\mathbf{r})]\mathbf{u}_T(\mathbf{r},z) \end{aligned} \tag{50}$$

B. Self-consistent Born approximation

As in the case of the scalar model, the SCBA and the CPA, (see next subsection) serve to calculate the frequency dependence of the reduced frequency-dependent shear modulus

$$\begin{aligned} Q(z) &= G(z)/\rho = Q'(\omega) - iQ''(\omega) \\ &= v_T(z)^2 = \widetilde{G}_0 - \Sigma(z) \end{aligned} \tag{51}$$

[1] As locally the translational and rotational invariance is broken one should in principle work with the full fourth-rank Hooke tensor $C_{ijkl}(\mathbf{r})$ instead of equation (46). The latter is an approximation to keep the model tractable.

and longitudinal modulus

$$\widetilde{M}(z) = M(z)/\rho = \widetilde{K} + \frac{4}{3}Q(z) = \widetilde{M}'(\omega) - i\widetilde{M}''(\omega)$$
$$= v_L(z)^2 = \widetilde{K} + \frac{4}{3}[\widetilde{G}_0 - \Sigma(z)] \quad (52)$$

which enter into macroscopic mean-field equations of motion

$$0 = -z^2 - \widetilde{M}(z)\nabla^2 \mathbf{u}_L(\mathbf{r}, z) \equiv A_L[z, \mathbf{r}, Q(z)]\mathbf{u}_L(\mathbf{r}, z) \quad (53)$$

$$0 = -z^2 - Q(z)\nabla^2 \mathbf{u}_T(\mathbf{r}, z) \equiv A_T[z, \mathbf{r}, Q(z)]\mathbf{u}_T(\mathbf{r}, z) \quad (54)$$

The effective action for deriving the SCBA is

$$S_{\rm eff}[\Sigma(z)] = S_{\rm med}[\Sigma(z)] + S_{SCBA}[\Sigma(z)] \quad (55)$$

Here $S_{SCBA}[\Sigma(z)]$ is given by Eq. (19) with

$$\gamma = V_c\big\langle[\widetilde{G}(\mathbf{r}) - \widetilde{G}_0]^2\big\rangle \quad (56)$$

The difference from the scalar model is that we now deal with 3-dimensional vectors. Therefore the trace includes a sum over the 3 cartesian degrees of freedom. This means that one has to sum the longitudinal contribution once and that of the transverse twice. Explicitly $S_{\rm med}[\Sigma(z)]$ takes the form

$$S_{\rm med}[\Sigma(z)] = {\rm Tr}\ln\Big(A\big[z, Q(z)\big]\Big)$$
$$= \sum_{\mathbf{k}} \ln\Big(A_L\big[z, \mathbf{k}, \widetilde{G}_0 - \Sigma(z)\big]\Big)$$
$$+2\sum_{\mathbf{k}} \ln\Big(A_T\big[z, \mathbf{k}, \widetilde{G}_0 - \Sigma(z)\big]\Big) \quad (57)$$

If we now vary $S_{\rm eff}$ of Eq. (55) with respect to $\Sigma(z)$, i.e. $\frac{\partial S_{\rm eff}}{\partial \Sigma(z)} = 0$ we get

$$\Sigma(z) = \gamma\frac{k_\xi^3}{6\pi^2}\chi^\xi(z) \quad (58)$$

with

$$\chi^\xi(z) = \frac{4}{3}\chi_L^\xi(z) + 2\chi_T^\xi(z) \quad (59)$$

This weighted susceptibility is given in terms of the local longitudinal and transverse susceptibilities

$$\chi_{L,T}^\xi(z) = \frac{3}{k_\xi^3}\int_0^{k_\xi} dk k^2 \chi_{L,T}(k, z) \quad (60)$$

with the k dependent susceptibilities

$$\chi_{L,T}(k, z) = k^2 \mathsf{G}_{L,T}(k, z) = \frac{k^2}{-z^2 + k^2 v_{L,T}(z)^2} \quad (61)$$

$\mathsf{G}_{L,T}(k, z)$ are the longitudinal and transverse Green's functions[2] Eq. (58) together with Eqs. (51), (52), (59), (60), and (61) establish the self-consistent vector SCBA equations for calculating the frequency-dependent reduced shear modulus $Q(z)$, and from this the relevant measurable quantities:

- Vibrational density of states

$$g(\omega) = \frac{2\omega}{3\pi}\frac{3}{k_D^3}\int_0^{k_D} dk k^2\Big(\mathsf{G}_L''(k, \omega) + 2\mathsf{G}_T''(k, \omega)\Big) \quad (62)$$

- Specific heat

$$C(T) \propto \int_0^\infty d\omega g(\omega)(\omega/T)^2\frac{e^{\hbar\omega/k_BT}}{[e^{\hbar\omega/k_BT} - 1]^2} \quad (63)$$

- Longitudinal and transverse sound attenuation $\Gamma_{L,T}$

$$\Gamma_L(\omega) = \omega M''(\omega)/M'(\omega)$$
$$\Gamma_T(\omega) = \omega G''(\omega)/G'(\omega) \quad (64)$$
$$\Leftrightarrow \quad v_{L,T}(z)^2 = {\rm Re}\big\{v_{L,T}^2\big\}\big[1 - i\Gamma_{L,T}/\omega\big]$$

- Longitudinal and transverse mean-free paths $\ell_{L,T}$

$$\frac{1}{\ell_{L,T}(\omega)} = \frac{\Gamma_{L,T}(\omega)}{2v_{L,T}(0)} \quad (65)$$

- Thermal conductivity [22]

$$\kappa(T) \propto \int_0^\infty d\omega \ell_T(\omega)(\omega^4/T^2)\frac{e^{\hbar\omega/k_BT}}{[e^{\hbar\omega/k_BT} - 1]^2} \quad (66)$$

- Coherent inelastic neutron and X-ray scattering intensity

$$S(k, \omega) \propto \underbrace{\frac{1}{1 - e^{\hbar\omega/k_BT}}}_{n(\omega)+1}{\rm Im}\big\{\chi_L(k, \omega)\big\} \quad (67)$$

- Depolaritzed Raman scattering intensity [7, 146]

$$I_{VH}(\omega) \propto [n(\omega) + 1]{\rm Im}\big\{\chi^{k_p}(\omega)\big\} \quad (68)$$

It should be noted that the same susceptibility combination, namely $\chi^\xi(\omega)$, which enters into the SCBA equation (58), appears also in the Raman intensity, Eq. (68), albeit with a cutoff k_P given by the fluctuations of the pockels constants and not the elastic constants [7, 146].

It should further be noted that the Raman intensity is *not* given by the Shuker-Gammon formula $I_{VH}(\omega) \propto [n(\omega) + 1]g(\omega)/\omega$ [13]. If one divides the expression of Eq. (68) for $I_{VH}(\omega)$ by Shuker and Gammon's expression one obtains the frequency-dependent coupling constant $C(\omega)$, which had been inserted as additional factor into the Shuker-Gammon formula in order to reconcile neutron and Raman-scattering results for the vibrational DOS [14, 16, 146–149].

[2] We use sans serif for the Green's functions $\mathsf{G}_{L,T}(k, z)$ in order to distinguish them from the shear modulus G.

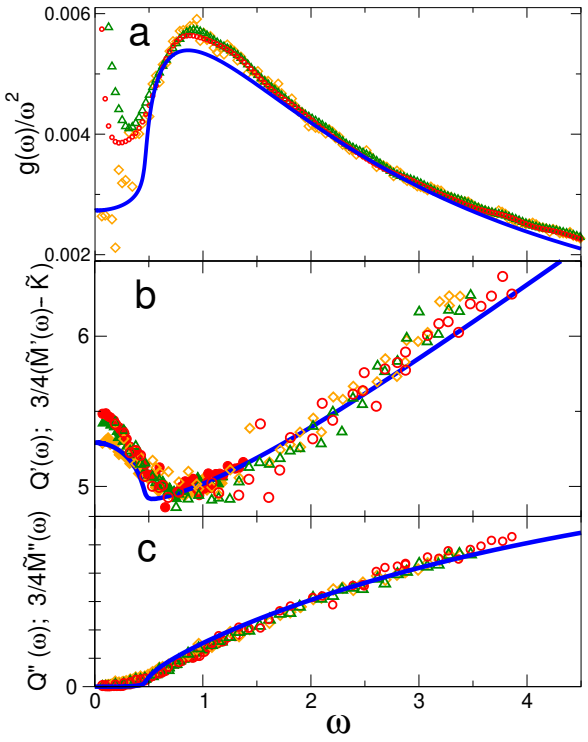

FIG. 5. Comparison of results of a soft-sphere molecular-dynamics simulation (symbols) with the prediction of heterogeneous-elasticity theory in self-consistent Born approximation (SCBA). We show the real parts (upper panel) and imaginary parts (lower panel) of the frequency-dependent shear modulus $G(\Omega_T)$ and the quantitity $3/4(M(\Omega_L)-\tilde{K})$ for three temperatures ($5{\cdot}10^{-3}$, $5{\cdot}10^{-4}$, $5{\cdot}10^{-5}$, in Lennard-Jones units) with $K = 30.4$. The SCBA parameters are $\gamma-\gamma_c = 0.08$ and $K/G_0 = 3.166$; from [38].

C. General features of the disorder-induced vibrational anomalies: Comparison of the SCBA version of heterogeneous-elasticity theory with a simulation

As stated in the introduction, the disorder-induced vibrational anomalies of glasses and other disordered solids feature three phenomena, which are related to each other

(*i*) The cross-over from Debye- to non-Debye behavior of the vibrational DOS, leading to a maximum in the reduced DOS $g(\omega)/\omega^2$, the boson peak;

(*ii*) a pronounced dip in the real part of the elastic coefficients (and their square-root, the frequency-dependent velocities) near the boson-peak frequency;

(*iii*) a strong increase of the sound attenuation below the boson-peak frequency (Rayleigh scattering), which enters into the imaginary parts of the elastic coefficients via Eq. (64).

These three anomalies are displayed in Fig. 5, in which the results of a molecular-dynamic simulation is compared with the prediction of heterogeneous-elasticity theory, solved in SCBA [38]. In this simulation a binary soft-sphere potential (i.e. a Kob-Andersen-type [150] binary Lennard-Jones potential without the attractive part) was taken for ten million particles. Such a potential mimics a metallic glass. The longitudinal and transverse frequency-dependent moduli were obtained from determining the longitudinal and transverse current correlation functions

$$C_{L,T}(k,\omega) = \frac{K_B T\omega}{\pi m}\mathsf{G}''(k,\omega) \tag{69}$$

where m is the paticles' mass. The simulation was run for three very different temperatures deep in the glassy state (see the figure caption). The very large particle number made it possible to avoid finite-size effect in the boson-peak frequency range. The data for the complex longitudinal modulus was converted to $Q(z) = G(z)/\rho$ via the inverse of Eq. (52)

$$Q(z) = \frac{3}{4}[\widetilde{M}(z) - \widetilde{K}] \tag{70}$$

in order to compare the data with the measured $Q(z)$. It is seen in the figure that – as the longitudinal and trasverse data ly on top of each other – the bulk modulus $\widetilde{K}$ indeed does not appreciably depend on frequency and correspondingly has a negligible imaginary part.

It is the strength of the present theory that it easily allows to explain how the three anomalies are related to each other. It was pointed out by Schirmacher et al. 2007 [117] that one can deduce from Eq. (62) and using the 3rd line of (64) a relation between the DOS and $\Gamma(\omega)$:

$$g(\omega) - g_D(\omega) \propto \Gamma(\omega) \propto \omega\Sigma''(\omega) \tag{71}$$

This means that the disorder-induced frequency dependence of the elastic coefficient, controlled by $\Sigma(\omega)$ is responsible for the boson peak. This can already understood using lowest-order perturbation theory, which leads to Rayleigh scattering.

On the other hand, the real parts and the imaginary parts of the frequency-dependent moduli are related to those of the response functions $\chi(z) = \chi'(\omega) - i\chi''(\omega)$. These have, due to the causality requirement (the answer must occur at a time later than the question), a one-to-one correspondence by the Kramers-Kronig relation [151]

$$\chi'(\omega) = \frac{1}{\pi}P\int_0^\infty d\bar{\omega}^2 \frac{\chi''(\bar{\omega})}{\bar{\omega}^2 - \omega^3} \tag{72}$$

This is most easily visualized by looking at the simulated data of the real and imaginary parts of $Q(z) = \widetilde{G}_0 - \Sigma(z)$, displayed in panels b and c. Usually the real part of an analytic function, such as $\chi^\xi(z)$, has a maximum near the bottom of the spectrum $[\chi^\xi]''(\omega)$ and a minimum near the top. Now, because not $Q(z)$ but $\Sigma(z)$ is proportional to $\chi^\xi(z)$ via the SCBA relation (58), $Q'(\omega)$ displays a *minimum* near the begin of the "disorder spectrum", or "random-matrix spectrum" $[\chi^\xi]''(\omega)$, obviously marked by the boson peak, displayed in panel a.

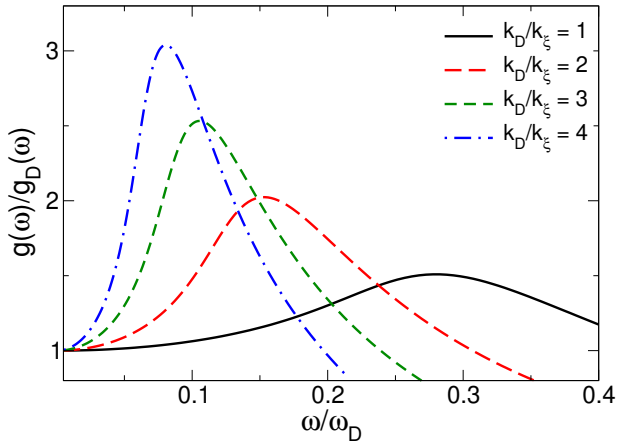

FIG. 6. Reduced density of states $g(\omega)/g_D(\omega)$ vs. the rescaled frequency $(\omega/\omega_D)(k_D/k_x i) = \omega/v_D k_\xi$ for different values of the ratio k_ξ/k_D. The other parameters are $\gamma/G_0^2 = 1$, $G_{\rm min} = 0$.

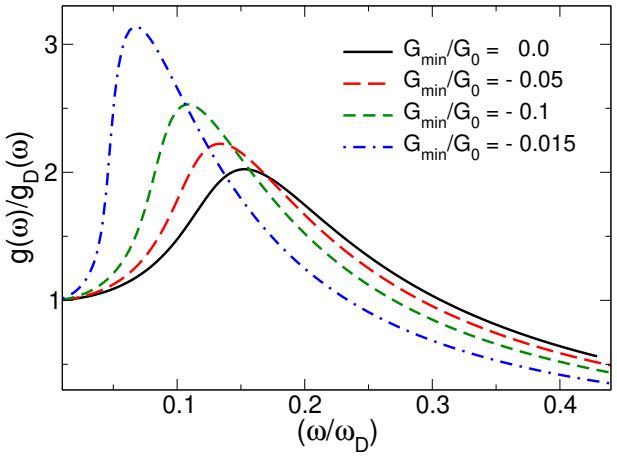

FIG. 7. Reduced density of states $g(\omega)/g_D(\omega)$ vs. the rescaled frequency (ω/ω_D) for different values of the lower cutoff $G_{\rm min}$ of the Gaussian distribution $P(G)$. The other parameters are $\gamma = /G_0^2 = 1.$, $k_D/k_\xi = 2$.

In the boson-peak regime and above, the data for very different temperatures collapse, which proves that the anomalies must be of harmonic origin. This is not so in the very low frequency regime, where anharmonic effects become visible [152, 153].

D. Coherent-Potential Approximation (CPA)

The vector CPA may be derived in the same way as the vector SCBA from the effective action

$$S_{\rm eff}[Q(z)] = S_{\rm med}[Q(z)] + S_{CPA}[Q(z)] \qquad (73)$$

where $S_{\rm med}[Q(z)]$ is given by Eq. (57) of the vector SCBA and $S_{CPA}[Q(z)]$ by Eq. (32) of the scalar CPA. The vector CPA equation takes the same form as the scalar one:

$$Q(z) = \left\langle \frac{\widetilde{G}_i}{1 + p\chi^\xi(z)[\widetilde{G}_i - Q(z)]} \right\rangle . \qquad (74)$$

but now with fluctuating shear moduli $\widetilde{G}_i$ and the vector version of $\chi^\xi(z)$, Eq. (59).

As in the scalar model the CPA has several advantages compared to the SCBA:

- one can treat arbitrary distributions $P(G)$;
- one is not restricted to weak disorder;
- one needs not (but can) take negative values of G into account.

For the calculations presented in Figs. 6 to 8 we used the CPA equation (74), together with (62) with a truncated Gaussian distribution of shear moduli of the form

$$P(G) = P_0\, \theta(G - G_{\rm min})\, e^{-(G-G_0)^2/2\gamma} \qquad (75)$$

where $\theta(x)$ is the Heaviside step function and $G_{\rm min}$ is the lower cutoff. In these calculations we used the *renormalized* value of G (i.e. the self-consistently calculated one) for evaluating the Debye frequency ω_D and Debye DOS $g_D(\omega)$ in terms of the longitudinal and transverse sound velocities $v_L^2 = K + \frac{4}{3}Q(0)$, $v_T^2 = Q(0)$

$$\omega_D = k_D \left[\frac{1}{3} \left(\frac{1}{v_L^3} + \frac{2}{v_T^3} \right) \right]^{-1/3} \qquad (76)$$

$$g_D(\omega) = 3\omega^2/\omega_D^3 \qquad (77)$$

For the bulk modulus of the calculations we used the value $K = 3.3G_0$ and for the cutoff parameter the value $\widetilde{\nu} = 1$, which implies $k_D/k_\xi = \sqrt[3]{3}\xi/a$, where $a = \sqrt[3]{V/N}$ is the mean intermolecular distance. The distribution of shear moduli (75) involves three parameters G_0, γ and $G_{\rm min}$. Because G_0 is used to fix the elastic-constant scale there remain three adjustable parameters to fix the *state of elastic disorder* of the material, namely $k_D/k_\xi \sim \xi/a$, γ and $G_{\rm min}$. The latter (which we used with negative values or equals zero) specify the amount of regions with negative shear modulus (soft regions) in the material. As can be seen from Figs. 6 to 8 increasing ξ and $|G_{\rm min}|$ enhances the BP *and* shifts its position to lower frequencies, whereas increasing γ just leads to an enhancement, while keeping the BP position constant. It has been pointed out in the literature [154–157] that the position of the boson peak in relation to the Debye frequency correlates with the inverse correlation length of density and elasticity fluctuations.

Let us discuss our findings further in terms of measured vibrational spectra of materials, in which an external parameter (temperature, pressure or the amount of polymerization) is changed. If the Debye frequency (depending on the moduli K and G) is changed, this leads to a modification of the spectrum, which has been called *elastic-medium transformation*. This transformation is

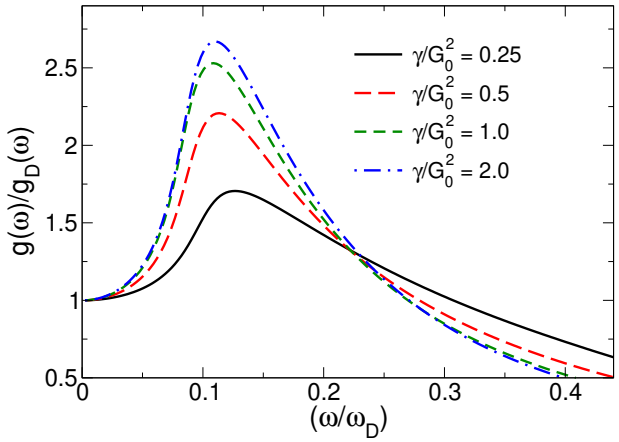

FIG. 8. Reduced density of states $g(\omega)/g_D(\omega)$ vs. the rescaled frequency (ω/ω_D) for different values of the width parameter γ. The other parameters are $G_{\min}/G_0 = -0.1$ and $k_D/k_\xi = 2$.

taken care of, if the DOS is represented in a normalized way, as is the case in Figs. 6 to 6. A number of boson-peak data, if normalized in this way, lead to a universal curve, i.e. all data points fall onto the same curve if re-plotted, taking the elastic transformation into account [32, 34, 59, 90, 92, 158**?**]. Other investigation reveal a *deviation* from this scaling [159–167]. In terms of our model calculations this means, if the state of disorder is not changed, but just the value of the mean elastic constants or the density, which go into the Debye frequency, this corresponds to elastic-transformation scaling. In the other cases obviously the state of disorder is changed by changing the external conditions.

A very interesting case in which the elastic transformation scaling does not hold has been reported recently: the case of prehistoric amber. [167] measured the temperature dependence of the specific heat of the hyperaged and rejuvenated material. The height of the boson peak, taken from a $C(T)/T^3$ curve is by 22 % lower in the hyperaged material, compared with the rejuvenated one. An elastic transformation using the change in the Debye frequency determined by the authors would only lead to a difference by 7.4 %.

IV. DISCUSSION AND CONCLUSIONS

Reading the text of the present article, one could be convinced that the boson peak in glasses and the associate vibrational anomalies can be satisfactory explained by the presence of the structural disorder, leading to spatial fluctuations of elastic coefficient, in particular the shear modulus. However, in the community working experimentally and theoretically on the vibrational properties of disordered and complex condensed matter there is no agreement about this. Whereas many authors agree, that the boson-peak-anomalies in glasses are due to the structural disorder, others maintain that this is not so and that the anomalies may be explained by conventional crystalline solid-state theory. Crystalline phonon theory is based on the phonon dispersions [168], reflecting the crystal symmetry group and anharmonic interactions, leading to renormalization and viscous damping [169–171].

As mentioned in the introduction, Chumakov et al. [90, 92] argue that the boson peak is "identical" [90] to a washed-out van-Hove singularity, i.e. just the result of the bending-over of the lowest (transverse) phonon dispersion near the first Brillouin zone. In fact, there is experimental evidence for crystal-like features in the spectrum of glasses and even liquids [172, 173]. These are caused by the short-range order, which is documented in the static structure factor $S(k)$ of glasses. The peak position k_0 of $S(k)$ corresponds to the diameter of the first Brillouin zone of a crystal. Correspondingly, $k_0/2$ corresponds to the radius of the Brillouin zone, where the phonon dispersions become horizontal and cause van-Hove singularities in the crystalline DOS.

In their inelastic X-Ray study of polycrystalline α-Quartz and glassy SiO_2, densified to match the crystalline density, accompanied with a numerical lattice-dynamics calculation of the crystalline phonon dispersions, Baldi et al. [173] find a crossover of the sound attenuation of the glass from a Rayleigh $\Gamma \propto \omega^4$ behaviour to a quadratic one at $\hbar\omega_c \sim 9$ meV, where the boson peak of densified silica has been reported [92]. At the same frequency the van-Hove singularity of the polycrystal is located. On the other hand, in the polycrystal, instead of Rayleigh scattering there is a linear behavior. Above ω_c the two attenuation coefficients match.

The interpretation of the authors is that below ω_c the glassy attenuation is due to elastic heterogeneities, above ω_c the spectrum is essentially the same of that of the polycrystal. These findings are certainly at variance with the claim that the boson-peak-type scenario leading to the $\Gamma \propto \omega^4 \to \omega^2$ crossover would have something to do with the bending-over of the transverse dispersion of the crystal. Obviously in this material the boson-peak frequency and the van-Hove-singularity are the same. This might also be the case for the other examples found by the authors of refs. [90, 92].

As indicated in the introduction, in the investigation of a two-dimensional macroscopic model glass the coexistence of crystal-like dispersions with the boson peak was observed [93], but the frequencies of the boson peak and that of the transverse van-Hove singularity are quite different. The boson peak was shown to show all salient features which identify its origin arising from the disorder. The conclusion is that the boson-peak, namely the disorder-induced peak in the reduced DOS is not "identical" with a washed-out van-Hove singularity. In some glasses their frequencies are just very near to each other.

In conclusion, the boson-peak related vibrational anomalies in glasses can consistently be explained by the presence of spatial fluctuations of elastic coefficients (elastic heterogeneity) with the help of the SCBA and CPA.

[1] S. R. Elliott, *The Physics of Amorphous Materials* (Longman, New York, 1984).
[2] K. Binder and W. Kob, *Glassy Materials and Disordered Solids: An Introduction* (World Scientific, London, 2011).
[3] See Refs. [2, 4–7] for recent reviews.,.
[4] T. Nakayama, Rep. Prog. Phys. **65**, 1195 (2002).
[5] M. Klinger, Phys. Reports **492**, 111 (2010).
[6] W. Schirmacher, phys. stat. sol. (b) **250**, 937 (2013).
[7] W. Schirmacher, T. Scopigno, and G. Ruocco, J. Noncryst. Sol. **407**, 133 (2014).
[8] P. Flubacher, A. J. Leadbetter, and J. A. Morris, J. Phys. Chem. Solids **12**, 53 (1959).
[9] A. J. Leadbetter and J. A. Morrison, Phys. Chem. Glasses **4**, 188 (1963).
[10] A. J. Leadbetter, Phys. Chem. Glasses **9**, 1 (1968).
[11] A. J. Leadbetter, J. Chem. Phys. **51**, 779 (1969).
[12] R. Shuker and R. W. Gammon, Phys. Rev. Lett. **25**, 222 (1970).
[13] R. Shuker and R. W. Gammon, in *Proceedings of the Second International Conference on Light Scattering in Solids*, edited by M. Balkanski (Flammarion, Paris, 1971) p. 334.
[14] J. Jäckle, in *Amorphous Solids:Low-Temmperature Properties*, edited by W. A. Phillips (Springer, Heidelberg, 1981) p. 135.
[15] A. J. Martin and W. Brenig, phys. status solidi (b) **64**, 163 (1974).
[16] B. Schmid and W. Schirmacher, Phys. Rev. Lett. **103**, 169702 (2009).
[17] U. Buchenau, N. Nücker, and A. J. Dianoux, Phys. Rev. Lett. **53**, 2316 (1984).
[18] J. Wuttke, W. Petry, G. Coddens, and F. Fujar, Phys. Rev. E **52**, 4026 (1995).
[19] A. I. Chumakov *et al.*, Phys. Rev. Lett. **92**, 245508 (2004).
[20] R. C. Zeller and R. O. Pohl, Phys. Rev. B **4**, 2029 (1971).
[21] J. J. Freeman and A. C. Anderson, Phys. Rev. B **34**, 2726 (1986).
[22] W. Schirmacher, Europhys. Lett. **73**, 892 (2006).
[23] W. A. Phillips, J. Low Temp. Phys. **7**, 351 (1972).
[24] P. W. Anderson, B. I. Halperin, and C. M. Varma, Philos. Mag. **25**, 1 (1972).
[25] W. Phillips, Rep. Prog. Phys. **50**, 1557 (1987).
[26] C. C. Yu and A. J. Leggett, Comm. Cond. Matter. Phys. **14**, 231 (1988).
[27] A. Würger, in *Springer Tracts in Modern Physics*, Vol. 135 (Springer, Heidelberg, 1996).
[28] S. Hunklinger and A. K. Raychaudhuri, in *Progress in Low-Temperature Physics*, Vol. 9, edited by D. F. Brewer (North-Holland, Amsterdam, 1986) p. 265.
[29] S. Hunklinger, in *Amorphous Insulators and Semiconductors*, edited by M. F. Thorpe and M. I. Mitkova.
[30] F. Sette, M. H. Krisch, C. Masciovecchio, G. Ruocco, and G. Monaco, Science **280**, 1550 (1998).
[31] G. Monaco and V. M. Giordano, PNAS **106**, 3659 (2009).
[32] G. Baldi, A. Fontana, G. Monaco, L. Orsingher, S. Rols, F. Rossi, and B. Ruta, Phys. Rev. Lett. **102**, 195502 (2009).
[33] G. Baldi, V. M. Giordano, G. Monaco, and B. Ruta, Phys. Rev. Lett. **104**, 195501 (2010).
[34] B. Ruta, G. Baldi, V. M. Giordano, L. Orsingher, S. Rols, F. Scarponi, and G. Monaco, J. Chem. Phys. **113**, 041101 (2010).
[35] G. Baldi, V. M. Giordano, and G. Monaco, Phys. Rev. B **83**, 174203 (2011).
[36] B. Ruta, G. Baldi, F. Scarponi, D. Fioretto, M. Giordano, and G. Monaco, J. Chem. Phys. **137**, 214502 (2012).
[37] G. Monaco and S. Mossa, PNAS **106**, 16907 (2009).
[38] A. Marruzzo, W. Schirmacher, A. Fratalocchi, and G. Ruocco, Scientific Reports **3**, 1407 (2013).
[39] V. G. Karpov, M. I. Klinger, and F. N. Ignatiev, Sov. Phys. JETP **84**, 760 (1983).
[40] U. Buchenau, Y. M. Galperin, V. L. Gurevich, and H. R. Schober, Phys. Rev. B **43**, 5039 (1991).
[41] See Refs. [5, 42] for the extended literature on soft potentials and quasi-local oscillators.,.
[42] H. R. Schober, U. Buchenau, and V. L. Gurevich, Phys. Rev. B **89**, 014204 (2014).
[43] V. L. Gurevich, D. A. Parshin, and H. R. Schober, Phys. Rev. B **67**, 094203 (2003).
[44] E. N. Economou, *Green's function in quantum physics* (Springer-Verlag, Heidelberg, 1971).
[45] A. L. Burin, L. A. Maksimov, and I. Y. Polishchuk, Physica B **210**, 15 (1995).
[46] E. Maurer and W. Schirmacher, J. Low-Temperature Phys. **137**, 453 (2004).
[47] W. Schirmacher, J. Non-Cryst. Sol. **357**, 518 (2011).
[48] S. Alexander and R. Orbach, J. Phys. (Paris) Lett. **43**, L625 (1982).
[49] B. Derrida, R. Orbach, and K.-W. Yu, Phys. Rev. B **29**, 6645 (1984).
[50] O. Entin-Wohlman, S. Alexander, R. Orbach, and K.-W. Yu, Phys. Rev. B **29**, 4588 (1984).
[51] S. Alexander, Physica **140A**, 397 (1986).
[52] T. Nakayama, K. Yakubo, and R. L. Orbach, Rev. Mod. Phys. **66**, 381 (1994).
[53] B. B. Mandelbrot, *The Fractal Geometry of Nature* (Freeman, New York, 1989).
[54] W. Schirmacher, in *Lecture Notes in Physics*, Vol. 887 (Springer, Heidelberg, 2015).
[55] I. Webman, Phys. Rev. Lett. **47**, 1496 (1981).
[56] S. Summerfield, Sol. State Comm. **39**, 401 (1981).
[57] T. Odagaki and M. Lax, Phys. Rev. B **24**, 5284 (1981).
[58] E. Courtens, J. Pelous, J. Phalippou, R. Vacher, and T. Woignier, Phys. Rev. Lett. **58**, 128 (1987).
[59] S. Caponi *et al.*, Phys. Rev. Lett. **102**, 027402 (2009).
[60] E. Akkermans and R. Maynard, Phys. Rev. B **32**, 7850 (1985).
[61] J. E. Graebner, B. Golding, and L. C. Allen, Phys. Rev. B **34**, 5696 (1986).
[62] A. F. Ioffe and A. R. Regel, Prog. Semicond. **4**, 237 (1960).
[63] N. F. Mott, *Metal-insulator transitions, 2nd Edition* (Taylor & Francis, London, 1990).
[64] E. Akkermans and R. Maynard, Phys. Rev. B **32**, 7850 (1985).
[65] S. John, H. Sompolinky, and M. J. Stephen, Phys. Rev. B **28**, 5592 (1983).
[66] P. B. Allen and J. L. Feldman, Phys. Rev. Lett. **62**, 645 (1989).
[67] W. Schirmacher and M. Wagener, Sol. State Comm. **86**, 597 (1993).
[68] W. Schirmacher, G. Diezemann, and C. Ganter, Phys.

Rev. Lett. **81**, 136 (1998).
[69] W. S. S. Pinski and R. A. Römer, Europhys. Lett. **97**, 16007 (2012).
[70] W. S. S. Pinski, T. Whall, and R. A. Römer, J. Condens. Matt. **24**, 405401 (2012).
[71] C. Tomaras and W. Schirmacher, J. Phys. Condens. Matter **25**, 495402 (2013).
[72] S. N. Taraskin and S. R. Elliott, J. Phys.: Condens. Matter **11**, A219 (1999).
[73] B. Rufflé, G. Guimbretière, E. Courtens, R. Vacher, and G. Monaco, Phys. Rev. Lett. **96**, 045502 (2006).
[74] H. Shintani and H. Tanaka, Nature Materials **7**, 870 (2008).
[75] M. Foret, E. Courtens, R. Vacher, and J.-B. Suck, Phys. Rev. Lett. **77**, 3831 (1996).
[76] M. Foret, E. Courtens, R. Vacher, and J.-B. Suck, Phys. Rev. Lett. **78**, 4669 (1997).
[77] E. Rat, M. Foret, E. Courtens, R. Vacher, and M. Arai, Phys. Rev. Lett. **83**, 1355 (1999).
[78] S. N. Taraskin and S. R. Elliott, Phys. Rev. B **61**, 12017 (2000).
[79] W. Schirmacher and M. Wagener, Philos. Mag. B **65**, 861 (1992).
[80] S. Alexander, J. Bernasconi, W. R. Schneider, and R. Orbach, Rev. Mod. Phys. **53**, 175 (1981).
[81] A. K. Jonscher, Nature **267**, 673 (1977).
[82] A. Long, Adv. Phys. **31**, 553 (1982).
[83] I. Webman, Phys. Rev. Lett. **47**, 1496 (1981).
[84] T. Odagaki and M. Lax, Phys. Rev. B **24**, 5284 (1981).
[85] S. Summerfield, Sol. State Comm. **39**, 401 (1981).
[86] M. L. Mehta, *Random Matrices*.
[87] F. M. Izrailev, Phys. Rep. **196**, 300 (1990).
[88] N. W. Ashcroft and N. D. Mermin, *Solid State Physics* (Saunders College, Philadelphia, 1976) p. 465.
[89] S. N. Taraskin, S. Elliott, Y. H. Loh, and G. Naturanjan, Phys. Ref. Lett. **86**, 1255 (2001).
[90] A. I. Chumakov *et al.*, Phys. Rev. Lett. **106**, 8519 (2011).
[91] R. Zorn, Physics **4**, 44 (2011).
[92] A. I. Chumakov *et al.*, Phys. Rev. Lett. **112** (2014).
[93] Y. Wang, L. Hong, Y. Wang, W. Schirmacher, and J. Zhang, Phys. Rev. B **98**, 174207 (2018).
[94] S. K. Sarkar, G. S. Matharoo, and A. Pandey, Phys. Rev. Lett. **92**, 215502 (2004).
[95] R. Kühn and U. Horstmann, Phys. Rev. Lett. **78**, 4067 (1997).
[96] M. Mézard, G. Parisi, and A. Zee, Nucl. Phys. B **559**, 689 (1999).
[97] V. Martín-Mayor, G. Parisi, and P. Verroccio, Phys. Rev. E **62**, 2373 (2000).
[98] T. S. Grigera, V. Martín-Mayor, G. Parisi, and P. Verrocchio, Phys. Rev. Lett. **87**, 085502 (2001).
[99] V. Martín-Mayor, M. Mézard, G. Parisi, and P. Verrocchio, J. Chem. Phys. **114**, 8068 (2001).
[100] T. S. Grigera, V. Martín-Mayor, G. Parisi, and P. Verrocchio, Nature **422**, 289 (2003).
[101] S. Ciliberti, T. S. Grigera, V. Martín-Mayor, G. Parisi, and P. Verrocchio, J. Chem. Phys. **119**, 8577 (2003).
[102] C. Ganter and W. Schirmacher, Philos. Magazine **91**, 1894 (2011).
[103] T. S. Grigera, V. Martín-Mayor, G. Parisi, P. Urbani, and P. Verrocchio, J. Statist. Mech: Theory and Experiment **2011**, P02015 (2011).
[104] Y. M. Beltukov, V. I. Kozub, and D. A. Parshin, Phys. Rev. B **87**, 134203 (2013).
[105] W. Götze and M. R. Mayr, Phys. Rev. E **61**, 578 (1999).
[106] U. Bengtzelius, W. Götze, and A. Sjölander, J. Phys. C **17**, 5915 (1984).
[107] W. Götze, *Complex Dynamics of Glass-Forming Liquids* (Oxford Univ. Press, Oxford, 2009).
[108] L. Landau and E. Lifshitz, *Theory of Elasticity* (Pergamon Press, 1959).
[109] A. J. McKane and M. Stone, Ann. Phys. (N. Y.) **131**, 36 (1981).
[110] J. P. Wittmer, A. Tanguy, J.-L. Barrat, and L. Lewis, Europhys. Lett. **57**, 423 (2002).
[111] F. L. eonforte, R. B. ere, A. Tanguy, J.-P. Wittmer, and J.-L. Barrat, Phys. Rev. B **72**, 224206 (2005).
[112] F. L. eonforte, A. Tanguy, J.-P. Wittmer, and J.-L. Barrat, Phys. Rev. Lett. **97**, 055501 (2006).
[113] M. T. A. Tanguy, C. Goldenberg, and J.-L. Barrat, Phys. Rev. B **80**, 026112 (2009).
[114] S. G. Mayr, Phys. Rev. B **79**, 060201 (2009).
[115] H. Mizuno, H. Mossa, and J.-L. Barrat, Europhys. Lett. **104**, 56001 (2013).
[116] A. Lemaître and C. Maloney, J. Statist. Phys. **123**, 415 (2006).
[117] W. Schirmacher, G. Ruocco, and T. Scopigno, Phys. Rev. Lett. **98**, 025501 (2007).
[118] W. Schirmacher, E. Maurer, and M. Pöhlmann, phys. stat. sol. (c) **1**, 17 (2004).
[119] C. Ganter and W. Schirmacher, Phys. Rev. B **82**, 094205 (2010).
[120] S. Köhler, R. Ruocco, and W. Schirmacher, Phys. Rev. B **88**, 064203 (2013).
[121] J. F. Lutsko, J. Appl. Phys. **65**, 2991 (1988).
[122] J. W. S. L. Rayleigh, Philos. Mag. **41**, 241 (1871).
[123] J. W. S. L. Rayleigh, Philos. Mag. **47**, 375 (1899).
[124] S. John and M. J. Stephen, Phys. Rev. B **28**, 6358 (1983).
[125] S. Gelin, H. Tanaka, and A. Lemaître, Nature Materials **15**, 1177 (2016).
[126] J. Hansen and I. McDonald, *Theory of Simple Liquids* (Elsevier Science, Amsterdam, 2006).
[127] W. Feller, *An Introduction to probability theory and its applications*, Vol. II.
[128] M. H. Ernst, J. Machta, J. R. Dorfman, and H., J. Statist. Phys. **34**, 413 (1984).
[129] J. Machta, M. H. Ernst, and H. van Beijeren and, J. Statist. Phys. **35**, 413 (1984).
[130] A. R. Long, J. McMillan, N. Balkan, and S. Summerfield, Philos. Mag. B **58**, 153 (1988).
[131] J. C. Dyre and T. B. Schrøder, Rev. Mod. Phys. **72**, 873 (2000).
[132] F. Wegner, Z. Phys. B **35**, 207 (1979).
[133] K. B. Efetov, I. L. A, and D. E. Khmelnitsk, Soviet Phys. JETP **52**, 568 (1980).
[134] L. Schäfer and F. Wegner, Zeitschrift für Physik B Condensed Matter **38**, 113 (1980).
[135] S. John, Phys. Rev. Lett. **58**, 2486 (1987).
[136] W. Schirmacher, B. Abaie, A. Mafi, G. Ruocco, and M. Leonetti, Phys. Rev. Lett. **120**, 067401.
[137] D. Vollhardt, AIP Conf. Proc. **1297**, 339 (2010).
[138] H. Böttger and V. V. Bryksin,.
[139] A. I. Efros and B. I. Shklovskiĭ, *Electronic properties of doped semiconductors* (Springer-Verlag, Heidelberg, 1984).
[140] P. Soven, Phys. Rev. **156**, 809 (1967).
[141] D. W. Taylor, Phys. Rev. **156**, 1017 (1967).
[142] H. Ebert, D. Ködderitzsch, and v. . . p. . . y. . . J. Minár, journal = Rep. Prog. Phys., .
[143] J. Wong and C. A. Angell, *Glass: Structure by Spec-*

troscopy (M. Dekker, New York, 1976).
[144] P. B. Allen, J. L. Feldman, and J. Fabian, Philos. Magazine B **79**, 1715 (1999).
[145] A. Ishimaru, *Wave propagation and scattering in random media, V* (Academic Press, New York, 1978).
[146] B. Schmid and W. Schirmacher, Phys. Rev. Lett. **100**, 137402 (2008).
[147] V. K. Malinovsky and A. P. Sokolov, Sol. St. Comm. **57**, 757 (1986).
[148] G. Viliani *et al.*, Phys. Rev. B **52**, 3346 (1995).
[149] V. N. Novikov and E. Duval, Phys. Rev. Lett. **103**, 169701 (2009).
[150] W. Kob and H. C. Andersen, Phys. Rev. Lett. **73**, 1376 (1994).
[151] J. D. Jackson, *Classical Electrodynamics* (Wiley, New York, 1962).
[152] A. Marruzzo, S. Köhler, A. Fratalocchi, G. Ruocco, and W. Schirmacher, Eur. Phys. J. Special Topics **216**, 83 (2013).
[153] C. Ferrante, E. Pontecorvo, G. Cerullo, A. Chiasera, G. Ruocco, W. Schirmacher, and T. Scopigno, Nature Comm. **4**, 1793 (2013).
[154] E. Duval, A. Boukenter, and T. Achibat, J. Phys. Condens. Matter **2**, 10227 (1990).
[155] S. R. Elliott, Europhys. Lett. **19**, 201 (1992).
[156] A. P. Sokolov *et al.*, Phys. Rev. Lett. **69**, 1540 (1992).
[157] L. Hong, V. N. Novikov, and A. P. Sokolov, J. Noncryst. Sol. **117**, 357 (2013).
[158] A. Monaco *et al.*, Phys. Rev. Lett. **97**, 135501 (2006).
[159] M. Zanatta *et al.*, Phys. Rev. B **81**, 212201 (2010).
[160] M. Zanatta *et al.*, J. Chem. Phys. **135**, 174506 (2011).
[161] L. Hong *et al.*, Phys. Rev. B **78**, 134201 (2008).
[162] S. Caponi *et al.*, Phys. Rev. B **76**, 092201 (2007).
[163] B. R. e, S. Ayrinhac, E. Courtens, R. Vacher, M. F. A. Wischnewski, and U. Buchenau, Phys. Rev. Lett. **104**, 067402 (2010).
[164] K. Niss *et al.*, Phys. Rev. Lett. **99**, 055502 (2007).
[165] L. Orsingher *et al.*, J. Chem. Phys. **132**, 124508 (2010).
[166] S. Corezzi *et al.*, J. Phys. Chem. B **117**, 14477 (2013).
[167] T. P.-C. neda *et al.*, Phys. Rev. Lett. **112**, 165901 (2014).
[168] A. A. Maradudin, E. W. Montroll, G. H. Weiss, and I. P. Ipatova, *Theory of lattice dynamics in the harmonic approximation, solid-state physics, Suppl.3* (Academic Press, New York, 1971).
[169] W. Götze and K. H. Michel, in *Dynamical Properties of Solids*, Vol. I., edited by G. K. Horton and A. A. Maradudin (North Holland, Amsterdam, 1974) Chap. 9.
[170] H. Horner, in *Dynamical Properties of Solids*, Vol. I., edited by G. K. Horton and A. A. Maradudin (North Holland, Amsterdam, 1974) Chap. 9.
[171] J. Scheipers and W. Schirmacher, Z. Phys. B **103**, 547 (1996).
[172] V. M. Giordano and G. Monaco, PNAS **107**, 21985 (2010).
[173] G. Baldi, M. Zanatta, E. Gilioli, V. Milman, K. Refson, B. Wehinger, B. Winkler, A. Fontana, and G. Monaco, Phys. Rev. Lett. **110**, 185503 (2013).